Author Manuscript

Author Manuscript

Author Manuscript

Author Manuscript

HHS Public Access

Author manuscript

J Phys Chem Lett. Author manuscript; available in PMC 2023 August 07.

Published in final edited form as:

J Phys Chem Lett. 2022 September 29; 13(38): 8833–8839. doi:10.1021/acs.jpclett.2c02126.

Charge of Phospholipids Determines the Rate of Lysozyme Aggregation but Not the Structure and Toxicity of Amyloid Aggregates

Kiryl Zhaliazka,
Department of Biochemistry and Biophysics, Texas A&M University, College Station, Texas 77843, United States

Stanislav Rizevsky,
Department of Biochemistry and Biophysics, Texas A&M University, College Station, Texas 77843, United States; Department of Biotechnology, Binh Duong University, Thu Dau Mot 820000, Vietnam

Mikhail Matveyenka,
Department of Biochemistry and Biophysics, Texas A&M University, College Station, Texas 77843, United States

Valeryia Serada,
Department of Biochemistry and Biophysics, Texas A&M University, College Station, Texas 77843, United States

Dmitry Kurouski
Department of Biochemistry and Biophysics, Texas A&M University, College Station, Texas 77843, United States; Department of Biomedical Engineering, Texas A&M University, College Station, Texas 77843, United States

Abstract

Biophysical properties of plasma membranes are determined by a chemical structure of phospholipids, including saturation of fatty acids and charge of polar heads of these molecules. Phospholipids not only determine fluidity and plasticity of membranes but also play an important role in abrupt aggregation of misfolded proteins. In this study, we investigate the role of the charge of the most abundant phospholipids in the plasma membrane on the aggregation properties of the lysozyme. We found that the charge of phospholipids determines the aggregation rate of

Corresponding Author: Dmitry Kurouski − Department of Biochemistry and Biophysics, Texas A&M University, College Station, Texas 77843, United States; Department of Biomedical Engineering, Texas A&M University, College Station, Texas 77843, United States; Phone: 979-458-3778; dkurouski@tamu.edu.

Supporting Information

The Supporting Information is available free of charge at https://pubs.acs.org/doi/10.1021/acs.jpclett.2c02126.

Height distribution of all analyzed aggregates; ATRFTIR and CD spectra of lysozyme aggregates grown in the lipid-free environment and in the presence of phospholipids; histogram of relative contributions of parallel β-sheet, unordered protein secondary structure, and antiparallel β-sheet in amide I of AFM-IR spectra collected from lysozyme fibrils grown in the lipid-free environment, as well as lysozyme aggregates grown in the presence of lipids (PDF)

Transparent Peer Review report available (PDF)

Complete contact information is available at: https://pubs.acs.org/10.1021/acs.jpclett.2c02126

The authors declare no competing financial interest.

Author Manuscript Author Manuscript Author Manuscript Author Manuscript

lysozyme and the morphology of the protein aggregates. However, the secondary structure and toxicity of these protein specimens are determined by the chemical nature rather than the charge of phospholipids. These findings show that the charge of phospholipids can be a key factor that determines the stability and aggregation mechanism of amyloidogenic proteins.

Graphical Abstract

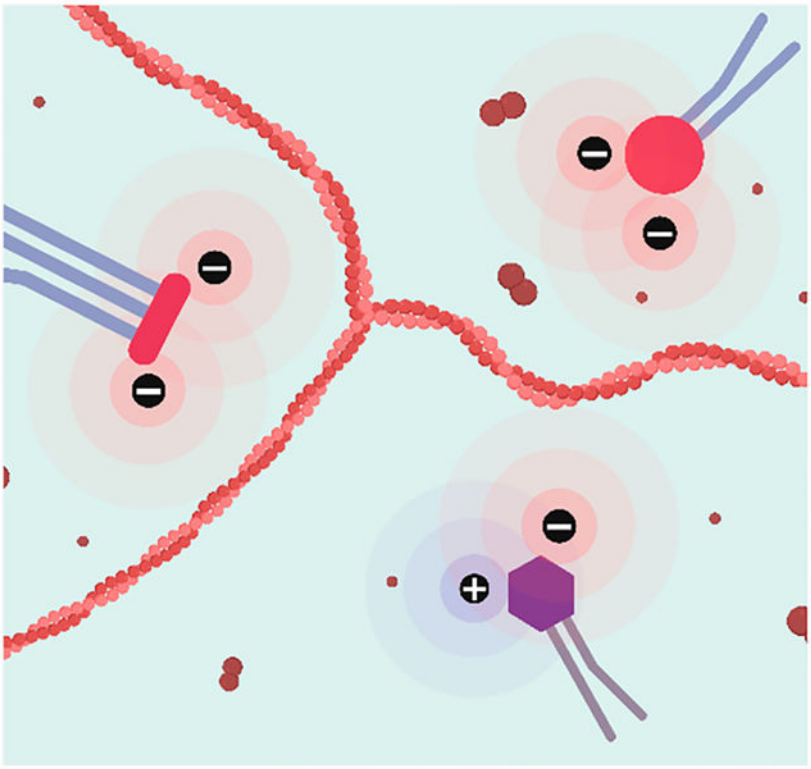

Plasma membranes perform a large number of physiologically important processes that range from cell division to transduction of ions and small molecules.[1,2] The incredible plasticity and functionality of membranes are attributed to a fine balance between carbohydrates, proteins, and lipids.[3] The vast majority of lipids found in the plasma membranes are phospholipids.[4] These molecules contain glycerol esterified to fatty acids (FAs) at *sn*-2 and *sn*-3 positions with the *sn*-1 position occupied by a phosphoric acid residue.[3,5] FAs can have a different number of carbon atoms and a degree of saturation.[1] The phosphoric acid residue may have no subsequent groups esterified to it (phosphatidic acid, PA) or can possess a broad variety of polar molecules such as choline (phosphatidylcholine, PC), ethanolamine (phosphatidylethanolamine, PE), serine (phosphatidylserine, PS), or phosphatidylglycerol, PG) (Scheme 1).[6,7]

Based on the net charge of the headgroup, all phospholipids can be divided into two big groups: zwitterions and anionic lipids (Scheme 1).[6,7] Zwitterions constitute around 75% of the lipid bilayer.[8] These molecules determine membrane plasticity and fludity.[3,9] Anionic lipids occupy significantly smaller volume of the plasma membrane. However, these lipids perform a large number of important physiological functions such as signal transition and

Author Manuscript Author Manuscript Author Manuscript Author Manuscript

cell apoptosis.[1,2] Cardiolipin (CL) is a unique phospholipid that constitutes ~20% of inner mitochondrial membrane.[6] It carries two negative charges playing an important role in cell respiration and energy conversion. Around 10% of the plasma membrane is occupied by PS. Under physiological conditions, negatively charged PS is primarily localized on the inner part of the membrane.[1,5,10] Its exposure to the exterior part of the plasma membrane indicates cell malfunction.[11] In such cases, PS is recognized by phagocytes that degrade such apoptotic and necrotic cells.[3] PG is present in plasma membranes in low amounts (only 1–2% of all phospholipids). However, PG is one of the most important lung surfactants that constitutes up to 11% of the surfactant lipids.[1,2]

Microscopic analysis of Lewy bodies, protein deposits that are found in midbrain, hypothalamus, and thalamus as a result of Parkinson's disease, revealed the presence of plasma membranes.[12] This finding suggests that lipids can be directly involved in the onset and development of neurodegenerative pathologies, such as Alzheimer's and Parkinson's diseases. Galvagnion and co-workers found that lipids can uniquely alter rates of protein aggregation. It was found that large unilamellar vesicles of phospholipids accelerated the rates of α-synuclein (α-syn) aggregation.[13–15] Similar findings were recently reported for amyloid β peptide islet amyloid precursor protein and insulin.[16–18] Furthermore, a growing body of evidence shows that lipids not only altered the rates of protein aggregation but also drastically changed the secondary structure of oligomers and fibrils, highly toxic protein aggregates that are linked to the onset and spread of neurodegenerative diseases.[19–23] Matveyenka and co-workers recently discovered that unsaturation of FAs of both PC and CL uniquely alters rates of insulin aggregation and determines the toxicity of insulin aggregates.[24] Similar findings were also observed for PS.[25] These results helped to understand the role of saturation of FAs in the phospholipids in the stability of amyloidogenic proteins. However, the role of the charge of the phospholipids remains unclear.

In this study, we investigate the effect of the charge of phospholipids on lysozyme aggregation. Abrupt aggregation of this protein is observed upon systemic amyloidosis.[26,27] We utilized a thioflavin T fluorescence approach to monitor the rate of lysozyme aggregation in the presence of two zwitterionic lipids, PC and PE, as well as anionic lipids with charges of negative one (PG) or negative two (CL). It should be noted that at the pH value of 3.0 used in our experiments, the carboxyl group of PS is protonated; therefore, this lipid possesses net positive charge (cationic lipid). Lysozyme was mixed with lipids at 1:5 molar rations. We also utilized atomic force microscopy (AFM) and the innovative nanoscale infrared spectroscopy, known as AFM-infrared (AFM-IR), to examine the morphologies and secondary structure of protein aggregates grown in the presence of these lipids.[28–30] Finally, we use mice midbrain N27 cells to investigate the extent to which zwitterionic, cationic, and anionic lipids altered the toxicity of lysozyme aggregates.[25]

In the lipid-free environment, lysozyme aggregation is characterized by a well-defined lag-phase (t_{lag} = 5.1 ± 0.6 h) that is followed by a rapid increase in the thioflavin T (ThT) fluorescence signal, which indicates the formation of protein aggregates (Figure 1). We found that both PS and PG drastically shortened t_{lag} of lysozyme aggregation. Specifically, Lys:PS t_{lag} was found to be 3.2 ± 0.2 h, whereas Lys:PG t_{lag}=4.1 ± 0.3h. We also found that

Author Manuscript Author Manuscript Author Manuscript Author Manuscript

in the presence of CL, lysozyme aggregated instantaneously with the shortest (t_{lag} = 0.2 ± 0.01 h) lag-phase. At the same time, our results showed that PC and PE strongly inhibited lysozyme aggregation. These findings point to the direct correlation between the net charge of the phospholipid and the t_{lag} of lysozyme aggregation. Specifically, CL with two negative charges enabled the strongest acceleration of lysozyme aggregation compared to PS and PG, which, in turn shortened the t_{lag} of lysozyme aggregation compared to the lipid-free environment. Finally, zwitterionic lipids fully inhibited protein aggregation.

We have also found that CL, PS, and PG enhanced the rate of lysozyme aggregation. Specifically, CL $t_{1/2}$ was 0.7 ± 0.1 h, whereas $t_{1/2}$ of PS and PG was 3.3 ± 0.2 h and 4.6 ± 0.2 h, respectively (Figure 1). It should be noted that $t_{1/2}$ of lysozyme in the lipid-free environment was 6.1 ± 0.5 h. Finally, we found that the intensities of Lys:CL, Lys:PG, and Lys:PS were greater than the intensity of lysozyme aggregates formed in the lipid-free environment. This finding suggests that insulin aggregation in the presence of cationic and anionic lipids yields more ThT active protein aggregates.

Next, we used AFM to investigate the morphology of lysozyme aggregates grown in the presence of zwitterionic, cationic, and anionic lipids, as well as in the lipid-free environment (Figure 2). We found that in the lipid-free environment, lysozyme formed both long and short fibrils with heights ranging from 20 to 40 nm (Figure 2). In the presence of PC, we observed predominantly small spherical aggregates that were 5–7 nm in height. We also observed a small amount of short fibril species in Lys:PC. However, only small oligomers were observed in Lys:PE. This observation is in good agreement with the above-discussed ThT results showing that PC and PE strongly inhibit lysozyme fibril formation yielding formation of only small oligomeric species. We also found that CL promotes formation of both small oligomers and prolonged fibrils that were ~20 nm in height, whereas predominantly fibrils were observed in the presence of PS. Finally, we found that in the presence of PG, lysozyme formed long fibrils that stretched to micrometers in length. Such long fibrils were not observed in any other sample. These findings show that charge of phospholipids determine the morphology of lysozyme aggregates. Specifically, in the presence of zwitterions, only oligomers are formed, whereas cationic and anionic lipids promote formation of fibrillar species. These results also show that in addition to the charge, the chemical structure of lipids plays an important role in the morphologies adopted by lysozyme aggregates. Specifically, the unique chemical structure of PG enabled lysozyme aggregation into long fibrils that were not observed for PS.

One may wonder whether in addition to the above-discussed morphological changes, the charge of phospholipids can also determine the secondary structure of Lys:PC, Lys:PE, Lys, PS, Lys:PG, and Lys:CL aggregates. Utilization of conventional optical techniques, such as attenuated total internal reflection Infrared spectroscopy (ATR-FTIR) and circular dichroism (CD), provides very little if any information about the secondary structure of protein aggregates. This is primarily due to the predominance of unaggregated protein and very low concentrations of protein aggregates (Figures S2 and S3). Therefore, to overcome this limitation, we used AFM-IR. This technique is based on thermal expansions in the analyzed sample that are induced by pulsed tunable IR light.[31–35] The expansions are recorded by the metallized scanning probe that can be precisely positioned on the surface

Author Manuscript Author Manuscript Author Manuscript Author Manuscript

of the object of interest.[36] Next, thermal expansions are converted into IR spectra that can be used to probe (i) secondary structure of protein specimens and (ii) composition of the analyzed aggregates.[22,28,37,38] Therefore, we used AFM-IR to examine the extent to which zwitterionic, cationic, and anionic lipids can change the secondary structure of lysozyme aggregates.

AFM-IR spectra collected from lysozyme fibrils grown in the lipid-free environment (Lys) are dominated by three vibrational bands centered around 1555 cm^{-1} (amide II) and 1630 and 1668 cm^{-1} (amide I). The position of amide I bands can be used to characterize protein secondary structure of the analyzed protein specimens.[29,39] Amide I band around 1630 cm^{-1} is indicative of parallel β-sheet, whereas the vibration around 1660 cm^{-1} is characteristic for unordered protein secondary structure. In the AFM-IR spectra of Lys, the 1630 cm^{-1} vibration was more intense than the 1668 cm^{-1} band (Figure S4). These results show that Lys fibrils grown in the lipid-free environment are composed of parallel β-sheet with significant contribution of unordered protein and antiparallel β-sheet present in their secondary structure (Figure S5).[39,40]

Lys:PE aggregates exhibit a similar spectroscopic fingerprint. Specifically, we observed both the intense 1630 cm^{-1} band and a weak 1668 cm^{-1} band in the AFM-IR spectra collected from Lys:PE oligomers. Considering this result, we can conclude that the secondary structures of Lys:PE are dominated by parallel β-sheet secondary structure (Figures S4 and S5).[39,40] However, a new set of vibrational bands was evident in the AFM-IR spectra collected from Lys:PE. Specifically, we observed intense vibrational bands around 800–900 and 1000–1200 cm^{-1}. These vibrational bands correspond to C−H and PO_2^- vibration of the ester group of lipids[37] (Figures 3 and S6). The presence of these vibrational bands in the AFM-IR spectra of Lys:PE shows that PE is present in the structure of these protein aggregates. Similar vibrational bands were observed in the AFM-IR spectra collected from Ins:PC oligomers. However, we found that the intensity of 800–900 and 1000–1200 cm^{-1} (PO_2^-) bands was significantly higher than the intensity of these bands in the spectrum of Ins:PE. These results show that Lys:PC possesses a higher amount of lipid than Lys:PE. We also found an ester (1730 cm^{-1}) vibration in the spectra collected from Ins:PC. These findings show that PE and PC have drastically different interactions with lysozyme in such oligomers. It is important to note that the amide I band of Lys:PC had significant changes compared to the amide I of Lys and Lys:PE. Specifically, we found the vibration at 1668 cm^{-1} to be more intense than the 1630 cm^{-1} band. These results show that Lys:PC oligomers are primarily composed of unordered protein and antiparallel β-sheet with some parallel β-sheet with some present in their secondary structure (Figure S5).[39,40]

We found that Lys:CL have similar secondary structure to Lys aggregates, Figure S3. Specifically, these fibrils were primarily composed of parallel and antiparallel β-sheet with some unordered protein present in their secondary structure.[39,40] Lys:PC and Lys:PG are dominated by parallel β-sheet, Figure S3. We also observed intense bands around 800–900, 1000–1200, and 1730 cm^{-1} in the AFM-IR spectra collected from Lys:PS, Lys:PG, and Lys:CL. These vibrational bands show that phospholipids are present in all of these protein aggregates.[37] Thus, we can conclude that cationic and anionic lipids induced only minor changes in the secondary structure of lysozyme aggregates. At the same time, the

Author Manuscript Author Manuscript Author Manuscript Author Manuscript

effect of zwitterionic lipids on the secondary structure of lysozyme aggregates formed in their presence in not uniform. Specifically, PC strongly altered the secondary structure of lysozyme oligomers, significantly reducing the amount of parallel β-sheet in these protein specimens. However, PE did not induce these drastic changes in the structure of Lys:PE oligomers compared to Lys fibrils. Finally, we can conclude that all protein aggregates that were grown in the presence of zwitterionic, cationic, and anionic lipids possess lipids in their structure.

These results resonate with the previously reported findings on the secondary structure of insulin oligomers and fibrils that were grown in the presence of PC, CL, and PS.[23–25] Specifically, Matveyenka and co-workers found that PC, CL, and PS were present in insulin aggregates that were grown in equimolar ratio with these lipids.[23–25] Similar findings were also reported by Dou and Kurouski for α-syn oligomers that were grown in the presence of PC.[22] Thus, we can conclude that lipid possession by protein aggregates that were formed in their presence can be considered a general phenomenon of amyloid biology.

It should be noted that some classes of aggregates, such as Lys:PE, Lys:PG, Lys:CL, and Lys, demonstrated very little if any structural heterogeneity of analysis aggregates (Figure S3). Lys:PC and Lys:PS exhibited a greater degree of structural heterogeneity, as can be observed in the acquired spectra. For instance, we observed two distinctly different types of AFM-IR spectra acquired from morphologically identical Lys:PS aggregates (Figure S3). These findings are in a good agreement with the previously reported AFM-IR analysis of insulin aggregates that were grown in the presence of PC and PS.[23–25] Additional studies are required to fully elucidate the observed heterogeneity of Lys:PC and Lys:PS, which are beyond the scope of the current work.

One may wonder whether the charge of phospholipids plays an important role in determination of toxicity of lysozyme aggregates that were grown in the presence of zwitterionic, cationic, and anionic lipids. To answer this question, we performed an LDH assay on mice midbrain N27 cells (Figure 4).[25] We found that the toxicity of Lys:PC and Lys:PE was significantly lower than the toxicity exerted by Lys fibrils. Furthermore, we found that Lys:PC was far less toxic than Lys:PE. Lys:PS, Lys:PG, and Lys:CL exhibited levels of cell toxicity similar to each other, which, in turn, were significantly lower than the toxicity of Lys aggregates. Thus, we can conclude that lipids present in the structure of Lys:PC, Lys:PE, Lys, PS, Lys:PG, and Lys:CL aggregates enabled the significant reduction of toxicity of these protein aggregates. Our results also show that there is no significant difference in the toxicity exerted by lysozyme aggregates grown in the presence of zwitterionic, cationic, and anionic lipids. It should be noted that the significantly lower cell toxicity of Lys:PC compared to all other samples can be attributed to both the unique chemical structure of PC and the low amount of parallel β-sheet present in these aggregates. Thus, the chemical structure of the lipid itself rather than the possessed charge determines the toxicity of protein aggregates that were grown in the presence of phospholipids.

Amyloid aggregates exert toxicities activating reaction oxygen species (ROS) production in cells.[41,42] These toxic species can also induce mitochondrial dysfunction in cells.[23–25] Therefore, we investigated the extent to which Lys:PC, Lys:PE, Lys, PS, Lys:PG, and

Author Manuscript Author Manuscript Author Manuscript Author Manuscript

Lys:CL, as well lysozyme fibrils grown in the lipid-free environment were engaged in ROS production and mitochondrial dysfunction of mice midbrain N27 cells (Figure 4). We found that ROS levels exerted by Lys:PC, Lys:PS, and Lys:PG were similar to the levels of ROS observed for Lys fibrils. However, Lys:PE and Lys:CL exerted significantly less ROS stress to N27 cells. Similar results were observed for level of mitochondrial dysfunction caused by these protein aggregates. Mitochondrial dysfunction can be determined using JC-1 assay.[24,25] Specifically, the presence of PC, PE, PS, and PG lipids did not significantly alter the extent to which lysozyme aggregates induce mitochondrial dysfunction. However, the presence of CL allowed for the significant reduction of the level of toxicity exerted by these protein aggregates to mitochondria. On the basis of this, we can conclude that ROS and JC-1 levels are determined by the chemical structure of the lipid rather than the charge present on its headgroup.

This conclusion is further supported by ROS levels and mitochondrial dysfunction expressed by the lipids themselves in mice midbrain N27 cells. Specifically, we found that PC, PE, and PG were inducing higher levels of ROS stress than PS and CL. We also observed that PG itself exerted significantly higher levels of mitochondrial dysfunction compared to all other lipids.

Summarizing, our results revealed a strong correlation between the rate of lysozyme aggregation and the charge of the phospholipid head. Specifically, zwitterions strongly inhibited fibril formation, whereas negatively charged PS, CL, and PG accelerated lysozyme aggregation. Furthermore, the acceleration rate was directly dependent on the net charge possessed by the lipids. We also found a direct relationship between the charge of the phospholipid head and the morphology of the protein aggregates formed in the presence of lipids. Specifically, in the presence of PC and PE, we found primarily small oligomers. However, in the presence of negatively charged phospholipids, domination of fibril-like aggregates was observed. Analysis of the secondary structure and toxicity exerted by Ins:PC, Ins:PE, Ins:PS, and Ins:PG revealed that the secondary structure and toxicity are determined by the chemical structure rather than by the charge of the phospholipid polar head. These results help to understand the importance of zwitterions in the plasma membrane. We infer that neutrally charged PC and PE stabilize proteins, preventing their fibrillization. Our findings also show that an increase in the concentration of cationic and anionic lipids in the plasma and mitochondrial membrane will promote the aggregation of misfolded proteins into fibrils, which, in turn, will activate ROS production and cause mitochondrial damage in cells.

Supplementary Material

Refer to Web version on PubMed Central for supplementary material.

ACKNOWLEDGMENTS

We are grateful to the National Institute of Health for the provided financial support (R35GM142869). The TOC graphic was created with BioRender.com software.

Author Manuscript Author Manuscript Author Manuscript Author Manuscript

REFERENCES

(1). van Meer G; Voelker DR; Feigenson GW Membrane lipids: where they are and how they behave. Nat. Rev. Mol. Cell Biol 2008, 9 (2), 112–24. [PubMed: 18216768]

(2). Fahy E; Subramaniam S; Murphy RC; Nishijima M; Raetz CR; Shimizu T; Spener F; van Meer G; Wakelam MJ; Dennis EA Update of the LIPID MAPS comprehensive classification system for lipids. J. Lipid Res 2009, 50 (Suppl), S9–14. [PubMed: 19098281]

(3). Fitzner D; Bader JM; Penkert H; Bergner CG; Su M; Weil MT; Surma MA; Mann M; Klose C; Simons M Cell-Type- and Brain-Region-Resolved Mouse Brain Lipidome. Cell Rep 2020, 32 (11), 108132. [PubMed: 32937123]

(4). Scollo F; Tempra C; Lolicato F; Sciacca MFM; Raudino A; Milardi D; La Rosa C Phospholipids Critical Micellar Concentrations Trigger Different Mechanisms of Intrinsically Disordered Proteins Interaction with Model Membranes. J. Phys. Chem. Lett 2018, 9 (17), 5125–5129. [PubMed: 30133296]

(5). Michaelson DM; Barkai G; Barenholz Y Asymmetry of lipid organization in cholinergic synaptic vesicle membranes. Biochem. J 1983, 211 (1), 155–62. [PubMed: 6870819]

(6). Pope S; Land JM; Heales SJ Oxidative stress and mitochondrial dysfunction in neurodegeneration; cardiolipin a critical target? Biochim. Biophys. Acta 2008, 1777 (7–8), 794–9. [PubMed: 18420023]

(7). Falabella M; Vernon HJ; Hanna MG; Claypool SM; Pitceathly RDS Cardiolipin, Mitochondria, and Neurological Disease. Trends Endocrinol. Metab 2021, 32 (4), 224–237. [PubMed: 33640250]

(8). Stace CL; Ktistakis NT Phosphatidic acid- and phosphatidylserine-binding proteins. Biochim. Biophys. Acta 2006, 1761, 913–926. [PubMed: 16624617]

(9). Mizuno S; Sasai H; Kume A; Takahashi D; Satoh M; Kado S; Sakane FDioleoyl-phosphatidic acid selectively binds to alpha-synuclein and strongly induces its aggregation. FEBS Lett 2017, 591 (5), 784–791. [PubMed: 28186641]

(10). Levental I; Levental KR; Heberle FA Lipid Rafts: Controversies Resolved, Mysteries Remain. Trends Cell. Biol 2020, 30 (5), 341–353. [PubMed: 32302547]

(11). Alecu I; Bennett SAL Dysregulated Lipid Metabolism and Its Role in alpha-Synucleinopathy in Parkinson's Disease. Front. Neurosci 2019, 13, 328. [PubMed: 31031582]

(12). Shahmoradian SH; Lewis AJ; Genoud C; Hench J; Moors TE; Navarro PP; Castano-Diez D; Schweighauser G; Graff-Meyer A; Goldie KN; Sutterlin R; Huisman E; Ingrassia A; Gier Y; Rozemuller AJM; Wang J; Paepe A; Erny J; Staempfli A; Hoernschemeyer J; Grosseruschkamp F; Niedieker D; El-Mashtoly SF; Quadri M; Van IWFJ; Bonifati V; Gerwert K; Bohrmann B; Frank S; Britschgi M; Stahlberg H; Van de Berg WDJ; Lauer ME Lewy pathology in Parkinson's disease consists of crowded organelles and lipid membranes. Nat. Neurosci 2019, 22 (7), 1099–1109. [PubMed: 31235907]

(13). Galvagnion C The Role of Lipids Interacting with -Synuclein in the Pathogenesis of Parkinson's Disease. J. Parkins. Dis 2017, 7, 433–450.

(14). Galvagnion C; Brown JW; Ouberai MM; Flagmeier P; Vendruscolo M; Buell AK; Sparr E; Dobson CM Chemical properties of lipids strongly affect the kinetics of the membraneinduced aggregation of alpha-synuclein. Proc. Natl. Acad. Sci. U. S. A 2016, 113 (26), 7065–70. [PubMed: 27298346]

(15). Galvagnion C; Buell AK; Meisl G; Michaels TC; Vendruscolo M; Knowles TP; Dobson CM Lipid vesicles trigger alpha-synuclein aggregation by stimulating primary nucleation. Nat. Chem. Biol 2015, 11 (3), 229–34. [PubMed: 25643172]

(16). Banerjee S; Sun Z; Hayden EY; Teplow DB; Lyubchenko YL Nanoscale Dynamics of Amyloid beta-42 Oligomers As Revealed by High-Speed Atomic Force Microscopy. ACS Nano 2017, 11 (12), 12202–12209. [PubMed: 29165985]

(17). Zhang Y; Hashemi M; Lv Z; Williams B; Popov KI; Dokholyan NV; Lyubchenko YL High-speed atomic force microscopy reveals structural dynamics of alpha-synuclein monomers and dimers. J. Chem. Phys 2018, 148 (12), 123322. [PubMed: 29604892]

Author Manuscript Author Manuscript Author Manuscript Author Manuscript

(18). Kakinen A; Xing Y; Hegoda Arachchi N; Javed I; Feng L; Faridi A; Douek AM; Sun Y; Kaslin J; Davis TP; Higgins MJ; Ding F; Ke PC Single-Molecular Heteroamyloidosis of Human Islet Amyloid Polypeptide. Nano Lett 2019, 19 (9), 6535–6546. [PubMed: 31455083]

(19). Chiti F; Dobson CM Protein Misfolding, Amyloid Formation, and Human Disease: A Summary of Progress Over the Last Decade. Annu. Rev. Biochem 2017, 86 (1), 27–68. [PubMed: 28498720]

(20). Knowles TP; Vendruscolo M; Dobson CM The amyloid state and its association with protein misfolding diseases. Nat. Rev 2014, 15 (6), 384–96.

(21). Iadanza MG; Jackson MP; Hewitt EW; Ranson NA; Radford SE A new era for understanding amyloid structures and disease. Nat. Rev. Mol. Cell Biol 2018, 19 (12), 755–773. [PubMed: 30237470]

(22). Dou T; Zhou L; Kurouski D Unravelling the Structural Organization of Individual alpha-Synuclein Oligomers Grown in the Presence of Phospholipids. J. Phys. Chem. Lett 2021, 12 (18), 4407–4414. [PubMed: 33945282]

(23). Rizevsky S; Matveyenka M; Kurouski D Nanoscale Structural Analysis of a Lipid-Driven Aggregation of Insulin. J. Phys. Chem. Lett 2022, 13 (10), 2467–2473. [PubMed: 35266717]

(24). Matveyenka M; Rizevsky S; Kurouski D Unsaturation in the Fatty Acids of Phospholipids Drastically Alters the Structure and Toxicity of Insulin Aggregates Grown in Their Presence. J. Phys. Chem. Lett 2022, 13, 4563–4569. [PubMed: 35580189]

(25). Matveyenka M; Rizevsky S; Kurouski D The degree of unsaturation of fatty acids in phosphatidylserine alters the rate of insulin aggregation and the structure and toxicity of amyloid aggregates. FEBS Lett 2022, 596, 1424–1433. [PubMed: 35510803]

(26). Pleyer C; Flesche J; Saeed F Lysozyme amyloidosis - a case report and review of the literature. Clin. Nephrol. Case Stud 2015, 3, 42–45. [PubMed: 29043133]

(27). Iqbal M; Jani P; Ahmed S; Sher T First Report of Hereditary Lysozyme Amyloidosis in a South Asian Family. Case Rep. Hematol 2019, 2019, 5092496. [PubMed: 30881710]

(28). Ruggeri FS; Longo G; Faggiano S; Lipiec E; Pastore A; Dietler G Infrared nanospectroscopy characterization of oligomeric and fibrillar aggregates during amyloid formation. Nat. Commun 2015, 6, 7831. [PubMed: 26215704]

(29). Ramer G; Ruggeri FS; Levin A; Knowles TPJ; Centrone A Determination of Polypeptide Conformation with Nanoscale Resolution in Water. ACS Nano 2018, 12 (7), 6612–6619. [PubMed: 29932670]

(30). Rizevsky S; Kurouski D Nanoscale Structural Organization of Insulin Fibril Polymorphs Revealed by Atomic Force Microscopy-Infrared Spectroscopy (AFM-IR). Chembiochem 2020, 21 (4), 481–485. [PubMed: 31299124]

(31). Dazzi A; Glotin F; Carminati R Theory of infrared nanospectroscopy by photothermal induced resonance. J. Appl. Phys 2010, 107 (12), 124519.

(32). Dazzi A; Prater CB AFM-IR: Technology and Applications in Nanoscale Infrared Spectroscopy and Chemical Imaging. Chem. Rev 2017, 117 (7), 5146–5173. [PubMed: 27958707]

(33). Kurouski D; Dazzi A; Zenobi R; Centrone A Infrared and Raman chemical imaging and spectroscopy at the nanoscale. Chem. Soc. Rev 2020, 49 (11), 3315–3347. [PubMed: 32424384]

(34). Katzenmeyer AM; Aksyuk V; Centrone A Nanoscale infrared spectroscopy: improving the spectral range of the photothermal induced resonance technique. Anal. Chem 2013, 85 (4), 1972–1979. [PubMed: 23363013]

(35). Katzenmeyer AM; Holland G; Kjoller K; Centrone A Absorption spectroscopy and imaging from the visible through midinfrared with 20 nm resolution. Anal. Chem 2015, 87 (6), 3154–3159. [PubMed: 25707296]

(36). Rizevsky S; Zhaliazka M; Dou T; Matveyenka M Characterization of Substrates and Surface-Enhancement in Atomic Force Microscopy Infrared (AFM-IR) Analysis of Amyloid Aggregates. J. Phys. Chem. C 2022, 126, 4157–4162.

(37). Dou T; Li Z; Zhang J; Evilevitch A; Kurouski D Nanoscale Structural Characterization of Individual Viral Particles Using Atomic Force Microscopy Infrared Spectroscopy (AFM-IR) and Tip-Enhanced Raman Spectroscopy (TERS). Anal. Chem 2020, 92 (16), 11297–11304. [PubMed: 32683857]

Author Manuscript Author Manuscript Author Manuscript Author Manuscript

(38). Ruggeri FS; Flagmeier P; Kumita JR; Meisl G; Chirgadze DY; Bongiovanni MN; Knowles TPJ; Dobson CM The Influence of Pathogenic Mutations in alpha-Synuclein on Biophysical and Structural Characteristics of Amyloid Fibrils. ACS Nano 2020, 14 (5), 5213–5222. [PubMed: 32159944]

(39). Kurouski D; Lombardi RA; Dukor RK; Lednev IK; Nafie LA Direct observation and pH control of reversed supramolecular chirality in insulin fibrils by vibrational circular dichroism. Chem. Commun 2010, 46 (38), 7154–6.

(40). Sarroukh R; Goormaghtigh E; Ruysschaert JM; Raussens V ATR-FTIR: a ″rejuvenated″ tool to investigate amyloid proteins. Biochim. Biophys. Acta 2013, 1828 (10), 2328–38. [PubMed: 23746423]

(41). Chen SW; Drakulic S; Deas E; Ouberai M; Aprile FA; Arranz R; Ness S; Roodveldt C; Guilliams T; De-Genst EJ; Klenerman D; Wood NW; Knowles TP; Alfonso C; Rivas G; Abramov AY; Valpuesta JM; Dobson CM; Cremades N Structural characterization of toxic oligomers that are kinetically trapped during alpha-synuclein fibril formation. Proc. Natl. Acad. Sci. U. S. A 2015, 112 (16), E1994–E2003. [PubMed: 25855634]

(42). Cataldi R; Chia S; Pisani K; Ruggeri FS; Xu CK; Sneideris T; Perni M; Sarwat S; Joshi P; Kumita JR; Linse S; Habchi J; Knowles TPJ; Mannini B; Dobson CM; Vendruscolo M A dopamine metabolite stabilizes neurotoxic amyloid-beta oligomers. Commun. Biol 2021, 4 (1), 19. [PubMed: 33398040]

Author Manuscript Author Manuscript Author Manuscript Author Manuscript

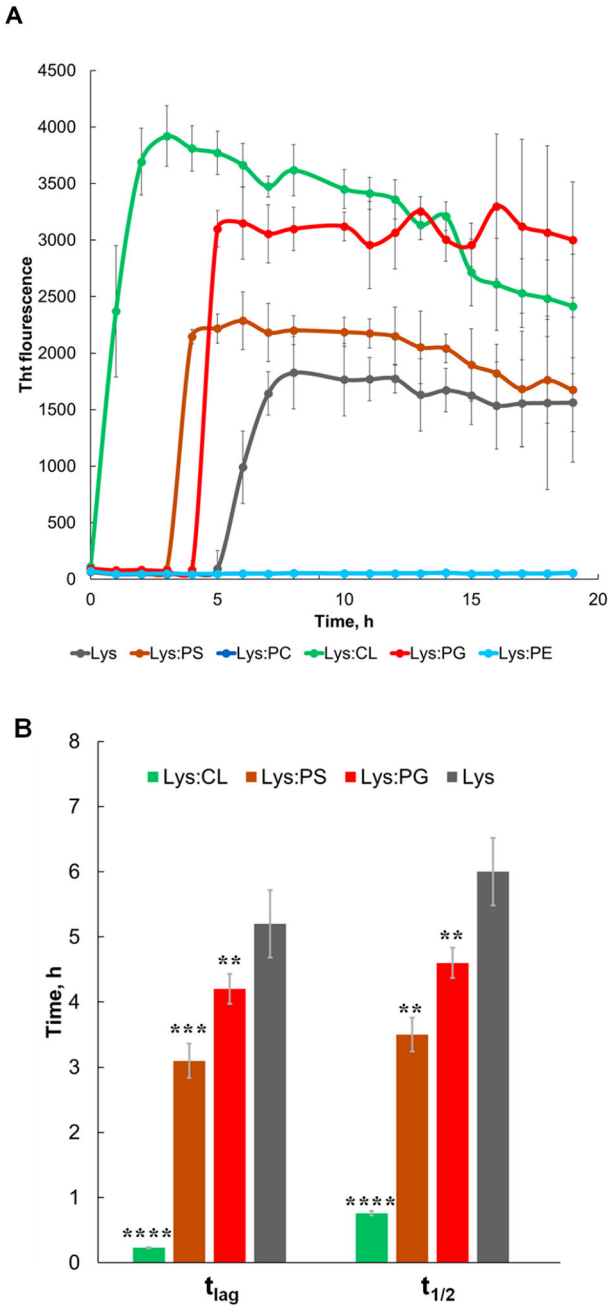

Figure 1.

Negatively charged phospholipids drastically accelerate, whereas zwitterionic phospholipids strongly inhibit lysozyme aggregation. (A) ThT aggregation kinetics with (B) corresponding values of t_{lag} and $t_{1/2}$ of lysozyme in the lipid-free environment (gray), as well as in the presence of PG (red), PS (brown), CL (green), PC (blue), and PE (light blue). Each kinetic curve is the average of three independent measurements.

Author Manuscript Author Manuscript Author Manuscript Author Manuscript

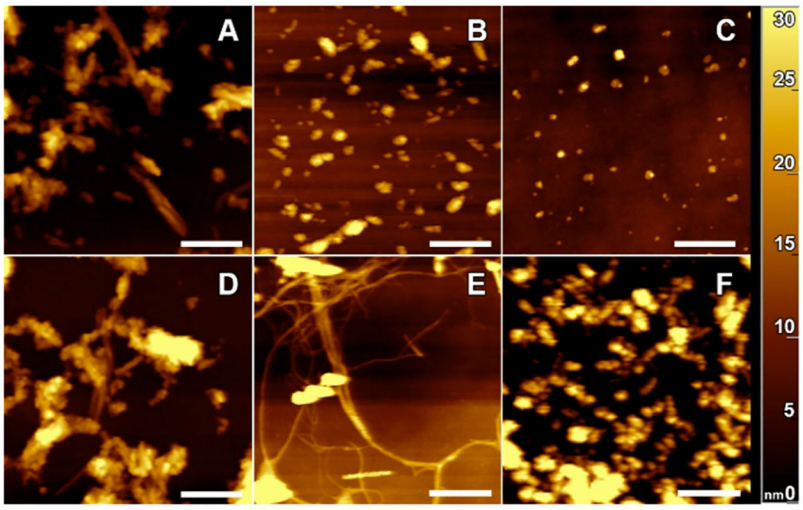

Figure 2.

Zwitterionic, cationic, and anionic phospholipids significantly alter morphologies of protein fibrils that form in their presence. AFM images of lysozyme fibrils grown in the lipid-free environment (A), as well as in the presence of PC (B), PE (C), PS (D), PG (E), and CL (F). Scale bars are 500 nm.

Author Manuscript Author Manuscript Author Manuscript Author Manuscript

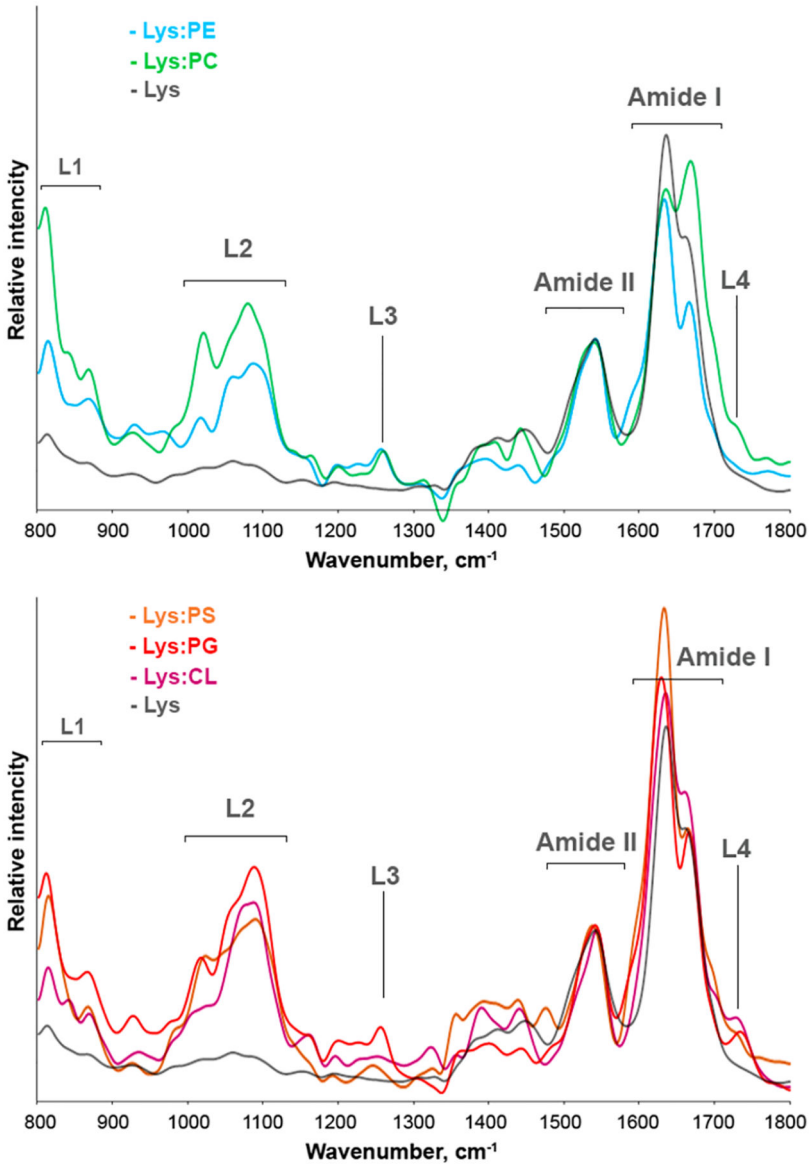

Figure 3.

Nanoscale analysis of secondary structure of lysozyme aggregates grown in the lipid-free environment and in the presence of phospholipids. Averaged AFM-IR spectra of Lys (gray), Lys:PC (green), Lys:PE (light blue), Lys:PS (orange), Lys:PG (red), and Lys:CL (purple) aggregates.

Author Manuscript Author Manuscript Author Manuscript Author Manuscript

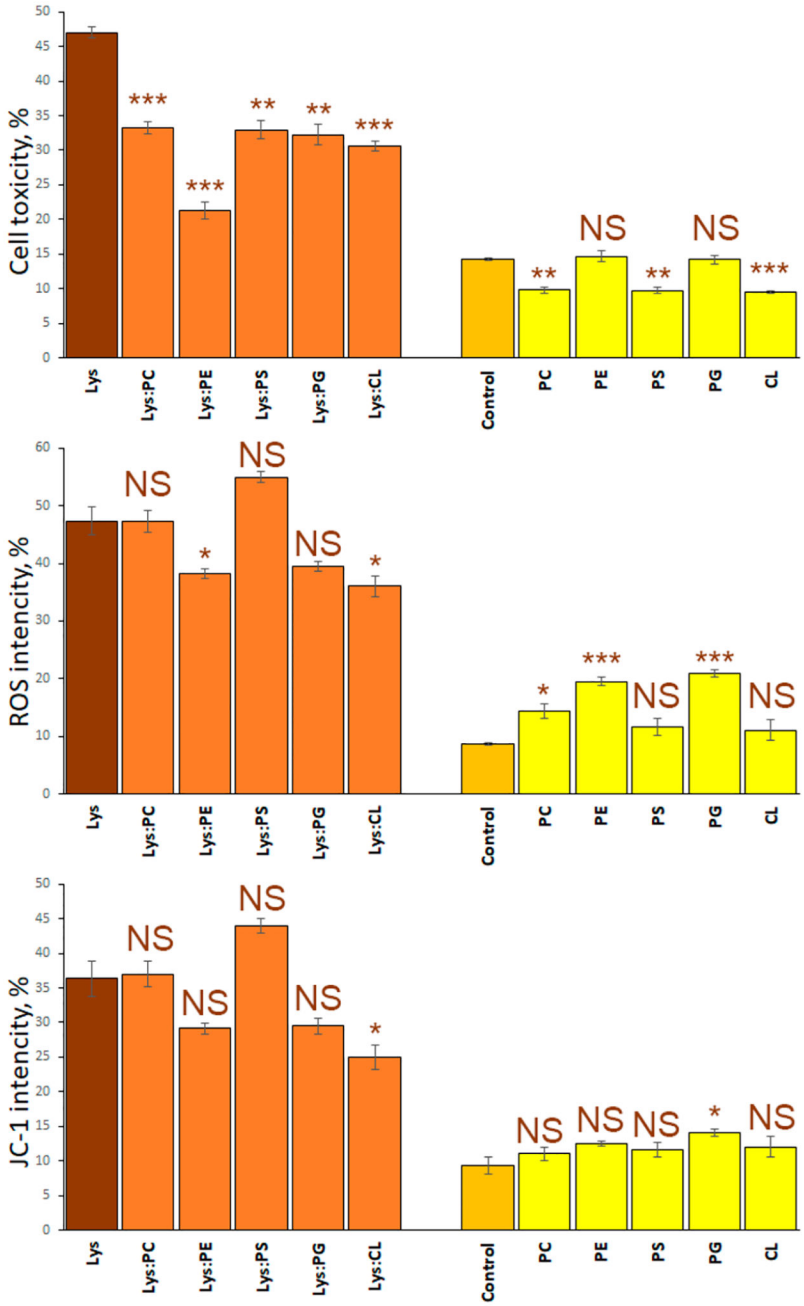

Figure 4.

Toxicity of lysozyme aggregates grown in the presence of lipids is determined by the chemical structure of the lipid. Histograms of LDH (top), ROS (middle), and JC-1 (bottom) toxicity assays of Lys (brown bars); Lys:PC, Lys:PE, Lys:PG, Lys:PS, Lys:CL (orange bars); and PC, PE, PG, PS, and CL (yellow bars). Error bars represent standard errors of the mean (SEM) of three replicates. According to the *t* test results, asterisks (*) show significance level of differences between Lys and lysozyme aggregates grown in the presence of lipids, as well as between the control and lipids themselves. NS is a nonsignificant difference, $*p \leq 0.05$; $**p \leq 0.01$, and $***p \leq 0.001$.

Author Manuscript Author Manuscript Author Manuscript Author Manuscript

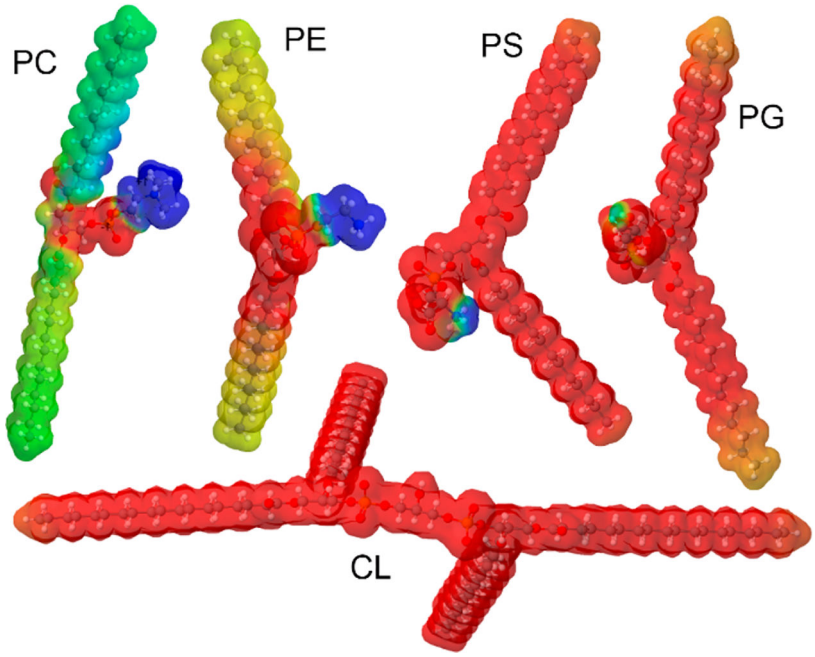

Scheme 1.

Molecular Structure of PC, PE, PS, PG, and CL with Their Electrostatic Potential that Illustrates Charge Distributions in These Phospholipids